Stress-Strain Characteristics of Foamed Concrete Subjected to Large Deformation under Uniaxial and Triaxial Compressive Loading

Xianjun Tan, Ph.D.[1]; Weizhong Chen, Ph.D.[2]; Hongyuan Liu, Ph.D.[3]; and Andrew Hin Cheong Chan, Ph.D.[4]

Abstract: Large compressive deformation associated with ideal plasticity-like stress plateaus is an extremely important performance characteristic of foamed concrete. However, there have been few investigations concerning the stress-strain characteristics of foamed concrete subjected to axial strain larger than 10% under uniaxial and triaxial compressive loading. In the current study, foamed concrete samples at three densities (250, 450, and 650 kg/m^3) were prepared and a series of tests were carried out. Axial stress-strain (σ_1-ε) curves were obtained, and peak stress (compressive strength), elastic modulus, peak strain, and the postpeak stress-strain relationship were analyzed. The experimental results showed that the stress-strain characteristics for foamed concrete at all three densities are similar and each can be ideally simplified into four stages. The compressive strength of foamed concrete increases with density and confining pressure, whereas elastic modulus has a positive correlation only with densities regardless of confining pressure. Additionally, no significant correlation was detected between peak strain and density, but peak strain increases with confining pressure. A linear relationship between residual compressive strength and strain was found for almost all test cases. Based on the experimental results, theoretical models for the prediction of peak stress, elastic modulus, and the postpeak stress-strain relationship were derived incorporating the effects of density and confining pressure.
DOI: 10.1061/(ASCE)MT.1943-5533.0002311.

Author keywords: Foamed concrete; Stress-strain characteristics; Large deformation; Triaxial compressive loading.

Introduction

Compared with conventional cement paste or concrete, foamed concrete, with its unique porous structure, has many advantages, such as its ability to sustain large deformation and its light weight, low cost, and good insulation. For these reasons, it is being used more and more widely in construction engineering and building for a number of different purposes (Narayanan and Ramamurthy 2000), including use as a raw material for precast lightweight blocks, cavity filling, thermal/fire and acoustic insulation, and road subgrade/widening (Ramamurthy et al. 2009; Amran et al. 2015). Furthermore, foamed concrete's large compressive deformation associated with the ideal plasticity-like stress plateau is a strong advantage that makes it perfect as a damping layer or energy absorber for densities between 400 and 1,600 kg/m^3 (Jones and Zheng 2013; Ahmad et al. 2009; Wang et al. 2012; Tan et al. 2017a). Foamed concrete has also been used as an aircraft-arresting system with densities between 275 and 337 kg/m^3 (Zhang et al. 2013). In most of these applications, the strength and deformation characteristics of foamed concrete play an important role. Therefore, it is necessary to study the stress-strain relationship of foamed concrete under various loading conditions.

To date, many investigations have been carried out to characterize the mechanical properties of foamed concrete under compressive loading (Narayanan and Ramamurthy 2000; Ramamurthy et al. 2009; Amran et al. 2015). The following sections discuss the main advantages of this material.

Compressive Strength

Amran et al. (2015) reported at least four factors that influence the compressive strength of foamed concrete.

- Pore characteristics, such as porosity (or density) and pore size, have a direct relationship with foamed concrete compressive strength. Several models of this relationship have been developed (Kearsley and Wainwright 2002; Rößler and Odler 1985; Hoff 1972; Chen et al. 2013; Lian et al. 2011).
- Constituent materials and mix proportions significantly influence foamed concrete compressive strength. Cement is essential (Kearsley and Wainwright 2001; Alexanderson 1979), supplemented by many different additives, such as fly ash (Kearsley and Wainwright 2001; Tan et al. 2014), bottom ash (Kim and Lee 2011; Qiao et al. 2008), fiber (Chen et al. 2012; Soleimanzadeh and Mydin 2013), sand (Jones and McCarthy 2005; Pan et al. 2007), silica fume (Chen et al. 2012; Pan et al. 2007), soil (Ma and Chen 2015), and oil palm shell (Yap et al. 2013; Shafigh et al. 2011). The water/cement (w/c) ratio is another important factor. An appropriate w/c ratio can increase

[1]Professor, State Key Laboratory of Geomechanics and Geotechnical Engineering, Institute of Rock and Soil Mechanics, Chinese Academy of Sciences, Wuhan, Hubei 430071, China (corresponding author). ORCID: https://orcid.org/0000-0001-8648-4437. Email: xjtan@whrsm.ac.cn

[2]Professor, State Key Laboratory of Geomechanics and Geotechnical Engineering, Institute of Rock and Soil Mechanics, Chinese Academy of Sciences, Wuhan, Hubei 430071, China. Email: wzchen@whrsm.ac.cn

[3]Senior Lecturer, School of Engineering and ICT, Univ. of Tasmania, Hobart, TAS 7001, Australia. Email: hong.liu@utas.edu.au

[4]Professor, School of Engineering and ICT, Univ. of Tasmania, Hobart, TAS 7001, Australia. Email: Andrew.Chan@utas.edu.au

Note. This manuscript was submitted on May 25, 2017; approved on December 19, 2017; published online on March 29, 2018. Discussion period open until August 29, 2018; separate discussions must be submitted for individual papers. This paper is part of the ***Journal of Materials in Civil Engineering***, © ASCE, ISSN 0899-1561.

the compressive strength of foamed concrete (Kearsley and Wainwright 2002; Tan et al. 2014; Jones and McCarthy 2005).
- Preparation method, age, size, and shape affect the compressive strength of foamed concrete (Tian et al. 2016; Kearsley and Wainwright 2002; Sim et al. 2013).
- Environmental factors, including high temperature and freezing-thawing, affect the compressive strength of foamed concrete (Mydin and Wang 2012; Othuman and Wang 2011; Sayadi et al. 2016; Tikalsky et al. 2014; Tan et al. 2013).

Elastic Modulus

Generally speaking, the elastic modulus (E) of foamed concrete is closely related to its compressive strength, so factors influencing one usually also affect the other. For example, foamed concrete with fly ash as a fine aggregate has been reported to exhibit a lower Young's modulus than that with sand (Jones 2001). Jones and McCarthy (2005) reported that the elastic moduli of the majority of their foamed concrete samples were significantly lower than those of their normal-weight concrete (NWC) and lightweight aggregate concrete (LWC) samples given equal compressive strength. The elastic moduli increased almost linearly with density. Tan et al. (2017b) indicated that an exponential function could be used to express the relationship of elastic modulus and density of foamed concrete, and introduced a model to reflect how damage to the elastic modulus varies with temperature. Similarly, Mydin (2012) obtained the elastic modulus–porosity relationship of foamed concrete at ambient temperatures, and concluded that Li and Purkiss's (2005) model can be used to predict the compressive modulus of elasticity at elevated temperatures.

Deformation Characteristics

Much research has focused on the stress-strain relationship for unconfined and confined NWC and LWC in compression, and various constitutive models have been put forward (Persson 2001; Nematzadeh et al. 2016; Wu et al. 2017; Jiang et al. 2017; Gabet et al. 2008; Attard and Setunge 1996; Wee et al. 1996; Lim and Ozbakkaloglu 2014; Zhou et al. 2016). However, relatively few studies on foamed concrete have been conducted. Mydin and Wang (2012) reported the effects of elavated temperature on the compressive stress-strain relationship of foamed concrete. They found that the strain corresponding to the peak strength increases with higher temperature and that the stress-strain curves are linear for stress up to 75% of peak strength for both NWC and LWC at all temperatures. Guo et al. (2015) conducted theoretical and experimental studies on the nonlinear mechanical properties of foamed concrete under uniaxial compression over the temperature range of −50 to 70°C and the strain rate range of 0.001–118/s. They developed an empirical model to describe this nonlinear deformation behavior. Ahmad Zaidi and Li (2009) studied the penetration resistance of lightweight foamed concrete subjected to impact by hard projectiles. They presented complete stress-strain curves in compression and determined several relevant parameters to describe the compressive strength and energy absorption of the foamed concrete.

Overall, numerous aspects of the mechanical properties of foamed concrete under compressive loading, especially for compressive strength, have been investigated. However, most of these properties were obtained under uniaxial compressive loading. Limited study has been devoted to triaxial compressive loading, although many applications are multiaxial, including the use of foamed concrete as a damping layer for large-deformation tunnels or roadways (Wang et al. 2012; Tan et al. 2017a). Furthermore, few studies have been carried out to obtain the stress-strain characteristics of foamed concrete subjected to strain greater than 10%, although this information would be beneficial for a number of broader applications.

The aim of the research reported in this paper was to establish the stress-strain characteristics of foamed concrete subjected to large deformation under uniaxial and triaxial compressive loading. For this purpose, foamed concrete specimens at three densities (250, 450, and 650 kg/m^3) were prepared and tested on a servo-controlled testing machine. Axial stress-strain ($\sigma_1 - \varepsilon$) curves for specimens at the different densities under uniaxial and triaxial loading conditions were obtained. Peak stress (compressive strength), elastic modulus, peak strain, and the postpeak stress-strain relationship were analyzed. Based on analysis results, theoretical models to predict peak stress, elastic modulus, and the postpeak stress-strain relationship were derived that include the effect of density and confining pressure.

Experimental Details

Materials and Mix Compositions

The cement used for the foamed concrete specimens was 425 portland cement per Chinese Standard GB175-2007 (National Standard of the People's Republic of China 2007). Because many studies have focused on the w/c ratio of foamed concrete (Amran et al. 2015), in order to highlight the influence of density on stress-strain characteristics in this work, the w/c ratio was kept constant at 0.45. Jones and Zheng (2013) concluded that all foamed concretes with densities of 400–1,600 kg/m^3 have excellent energy absorption. However, in aircraft-arresting systems the optimal density of foamed concrete is approximately 300 kg/m^3 (Zhang et al. 2013). Furthermore, when used in combination with U-shaped steel as a support system for underground coal mine roadways subjected to large deformations, the optimal density is approximately 500 kg/m^3 (Tan et al. 2017a). For these reasons, densities of 250, 450, and 650 kg/m^3 were chosen for use in this study. The mix proportion, designed according to dry density, is described next.

The amount of cement was calculated as

$$M_c = \frac{\rho_d}{S_a} \tag{1}$$

where, ρ_d = dry density of the foamed concrete; S_a = empirical coefficient (1.2 in this study); and M_c = mass of cement.

The amount of foaming agent was calculated as

$$M_p = \frac{\rho_f V_f}{\alpha + 1} = \frac{\rho_f K}{\alpha + 1}\left[1 - \left(\frac{M_c}{\rho_c} + \frac{M_w}{\rho_w}\right)\right] \tag{2}$$

where, M_p = mass of foaming agent; α = dilution ratio (20 in this study); ρ_f, ρ_c, and ρ_w = densities of foam, cement, and water, respectively (33.8, 3,100, and 1,000 kg/m^3, respectively); M_w = mass of water ($M_w = 0.45M_c$ because the w/c was kept constant at 0.45); and K = coefficient determined according to foam quality [1.1 in this study (Tan et al. 2017b)].

The mix proportions are summarized in Table 1.

Sample Preparation

The production process for the foamed concrete specimens was as follows:

1. Pretreatment and measurement—the cement was filtered by a 0.08-mm mesh sieve to remove hard blocks. The the cement and water were then measured.

Table 1. Mix proportions for different densities of foamed concrete

Mix code	Target density (kg/m^3)	Cement (kg/m^3)	Water (kg/m^3)	Foaming agent (kg/m^3)
M1	250	208.33	93.75	1.49
M2	450	375.00	168.75	1.26
M3	650	541.67	243.75	1.03

2. Foam preparation—the foaming agent and water, in proportions of 1:20, were poured into a foam generator. The foam was formed, and its specific volume was measured using a measuring glass.
3. Mixing—the measured cement and water were placed in a blender and mixed at low speed (30—40 rpm) to form a slurry. The chosen amounts of foam were added to the slurry, which was then mixed for 2–3 min at high-speed (60–120 rpm).
4. Pouring—when the cement-foam slurry was evenly mixed, it was poured into the molds. All densities were cast in plastic molds of of 600-mm length, 400-mm width, and 300-mm height. The prepared blocks were removed from the molds 24 h after casting and then seal-cured in a curing tank for 28 days.
5. Shaping—the blocks were removed and shaped to standard cylindrical specimens (Ø 50 mm × 100 mm). For each mix, 12 blocks were prepared. All of them were placed in drying oven at 105°C for 48 h before testing to make sure they were in the same condition for testing.

Test Procedures

The mass of each dried sample was measured at first. Twelve specimens of similar weight were chosen for each density, and three samples for each density were subjected to uniaxial compressive tests followed by triaxial tests at different confining pressures. Because there can be significant variation in the compressive strength of foamed concrete at different densities, it was not possible to apply the same confining pressure to all samples. Therefore, the confining pressure was derived as follows:

$$\sigma_3 = \alpha\sigma_c \tag{3}$$

where σ_3 = confining pressure; σ_c = uniaxial compressive strength of the foamed concrete at a given density; and α = scale parameter of the confining pressure and uniaxial compressive strength (0.25, 0.5, and 0.75 were used to represent the most common range of lateral pressure).

All compressive tests were carried out on a multifunction rock mechanics test (RMT) machine with a strain rate of 0.05/s. A schematic of the device is shown in Fig. 1. The RMT machine has a unique multifunction design and control technology that permits tests for different stress paths, such as uniaxial and triaxial compression, tension, shear, and fatigue. Its maximum load capacity is 1 MN and its maximum confining pressure is 50 MPa (Tan et al. 2013).

Results and Analysis

The axial stress-strain (σ_1-ε) curves for the three densities of foamed concrete specimens under uniaxial and triaxial conditions are shown in Figs. 2–4. It is observed that the stress-strain characteristics for all three densities are similar. They are ideally simplified as shown in Fig. 5 and explained as follows:

- oa_i ($i = 1, 2, 3, 4$) = elastic deformation stage;
- a_ib_i = plastic deformation stage; and b_i = peak stress (usually known as compressive strength);

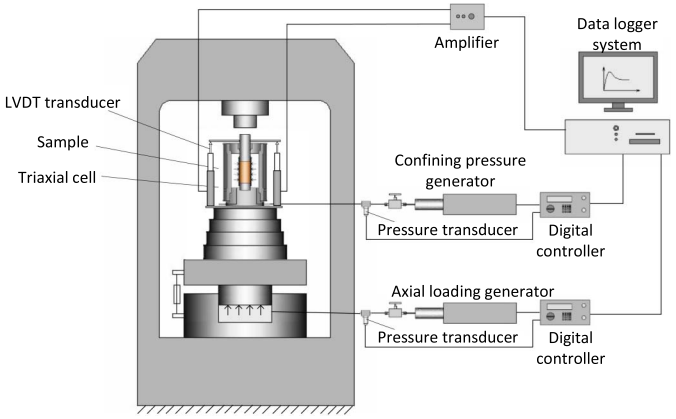

Fig. 1. Schematic of multifunction rock mechanics test machine.

- b_ic_i = post-peak strain softening stage; and c_i = beginning point of residual deformation; and
- c_id_i = residual deformation stage; and d_i = end point of stable residual deformation.

With the help of Fig. 5, much information can be obtained from Figs. 2–4, such as peak stress (or compressive strength), elastic modulus, peak strain, and the postpeak stress-strain relationship. The following sections provide detailed analysis of the variations in these characteristics.

Peak Stress

Variations in peak stress (or compressive strength) with density and confining pressure, as determined by the scale parameter α, are provided in Fig. 6. As expected, the compressive strength of foamed concrete increases with density and confining pressure. Linear regression was used to derive an equation for describing the quantitative relationships between peak strength and the ratio of confining pressure.

$$\sigma_{\text{peak}} = k_1 \times \alpha + \sigma_c \tag{4}$$

where σ_{peak} = peak stress or compressive strength (i.e., stress of point b_i in Fig. 5); and k_1 = increasing slope of peak stress with ratio of confining pressure. Both k_1 and σ_c are influenced by density as summarized in Table 2. From Table 2, the relationships among a, b, and density can be obtained. They are as follows:

$$\begin{aligned} k_1 &= 0.00001\rho^2 - 0.0045\rho + 0.693 (R^2 = 1) \\ \sigma_c &= 0.095e^{0.0054\rho} (R^2 = 0.99) \end{aligned} \tag{5}$$

where ρ = density of the foamed concrete.

Therefore, substituting Eq. (5) into Eq. (4) yields the peak stress in different densities and confining pressures.

$$\sigma_{\text{peak}} = (0.00001\rho^2 - 0.0045\rho + 0.693) \cdot \alpha + 0.095e^{0.0054\rho} \tag{6}$$

Elastic Modulus

Elastic modulus was taken as the tangent modulus at 50% of compressive strength. The experimental results for the variation in the elastic modulus of foamed concrete at different densities and confining pressures are shown in Fig. 7. Because the three duplicate tests in each series gave very consistent results, only the average value of each phase is provided.

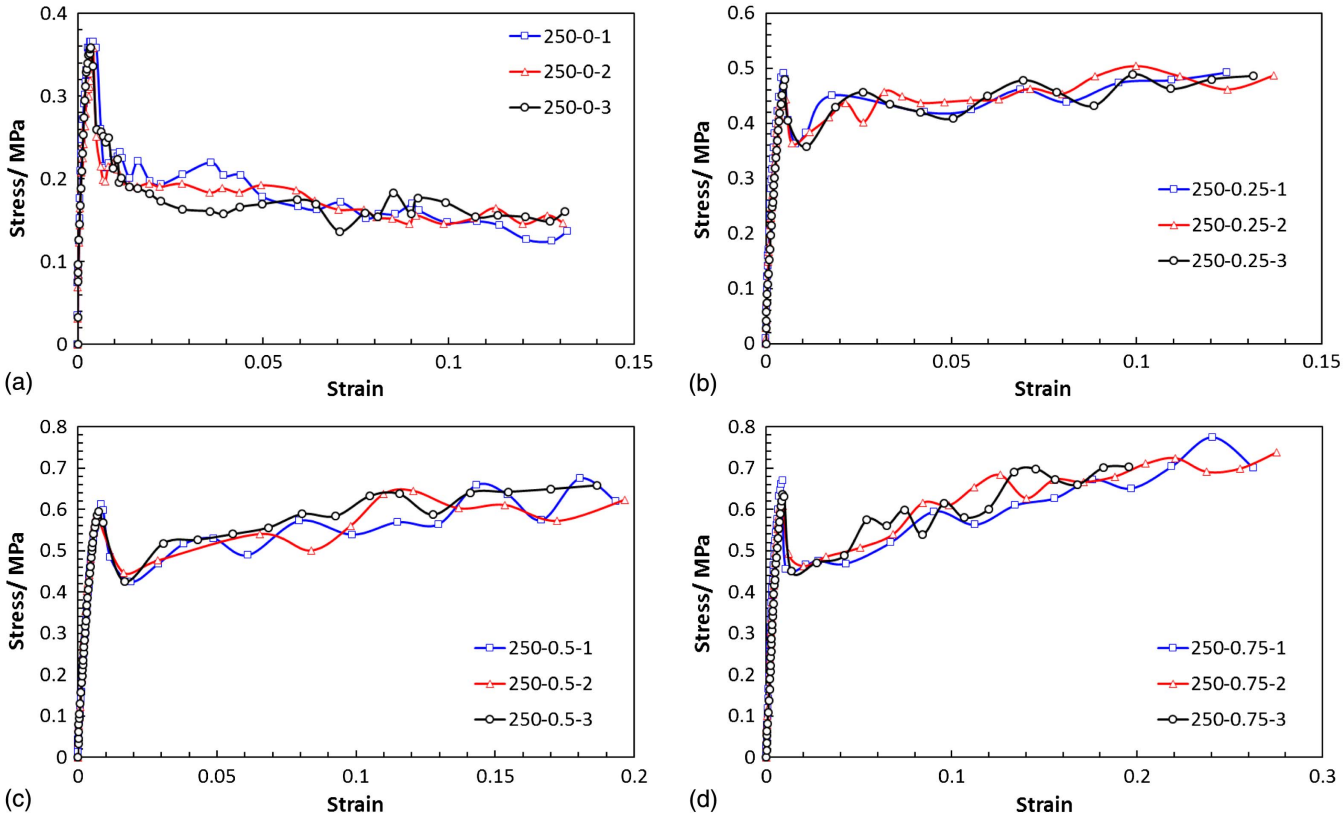

Fig. 2. Stress-strain curves for foamed concrete with 250-kg/m^3 density under uniaxial and triaxial compressive loading: (a) $\alpha = 0$; (b) $\alpha = 0.25$; (c) $\alpha = 0.5$; and (d) $\alpha = 0.75$.

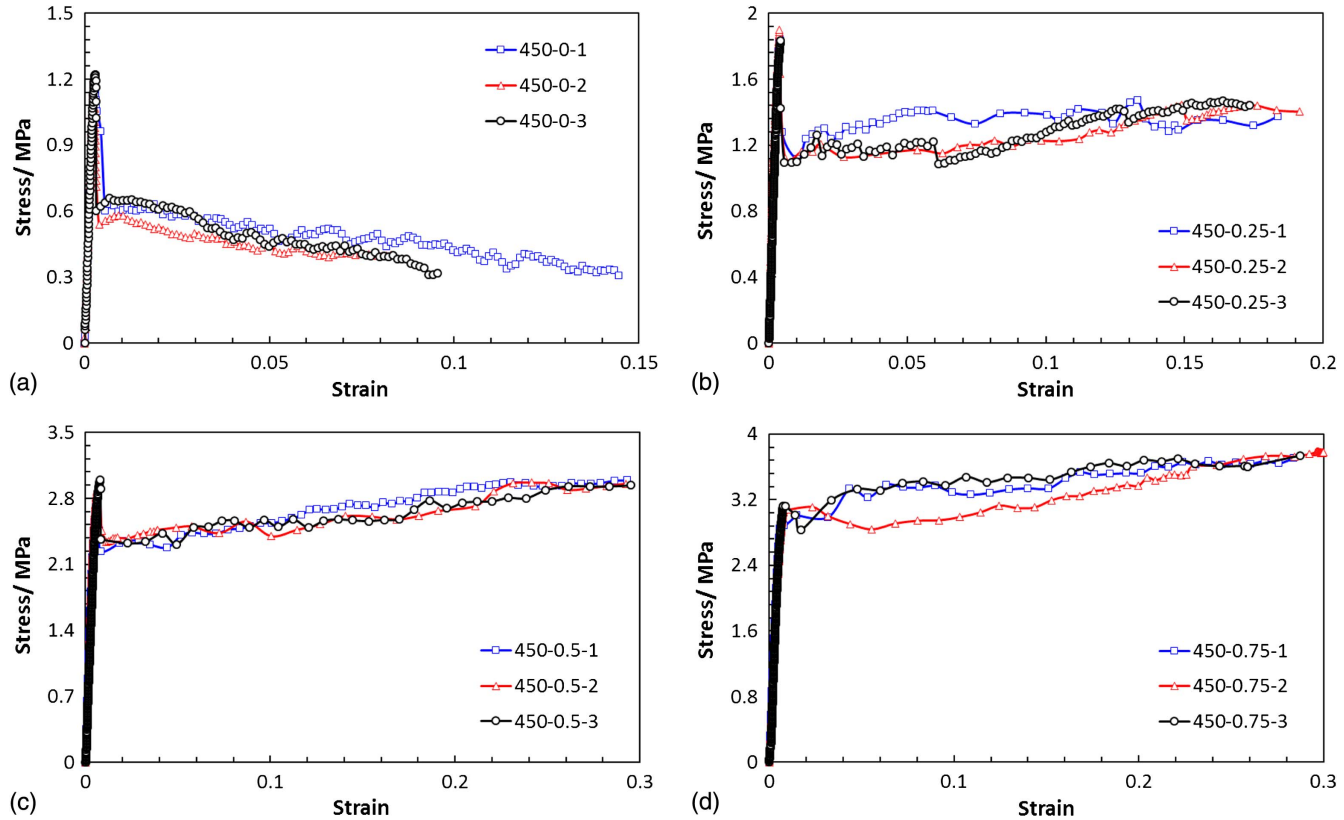

Fig. 3. Stress-strain curves for foamed concrete with 450-kg/m^3 density under uniaxial and triaxial compressive loading: (a) $\alpha = 0$; (b) $\alpha = 0.25$; (c) $\alpha = 0.5$; and (d) $\alpha = 0.75$.

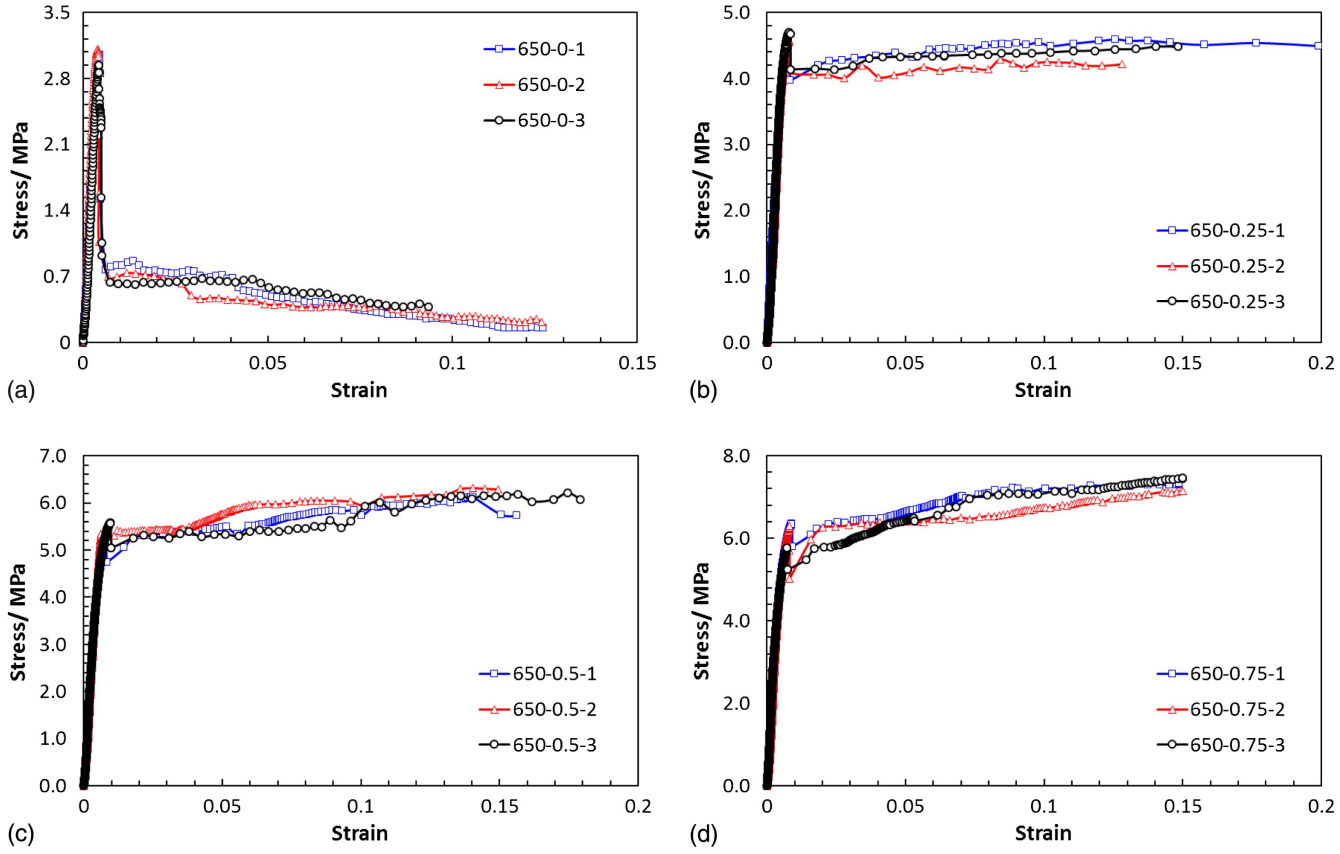

Fig. 4. Stress-strain curves for foamed concrete with 650-kg/m^3 density under uniaxial and triaxial compressive loading: (a) $\alpha = 0$; (b) $\alpha = 0.25$; (c) $\alpha = 0.5$; and (d) $\alpha = 0.75$.

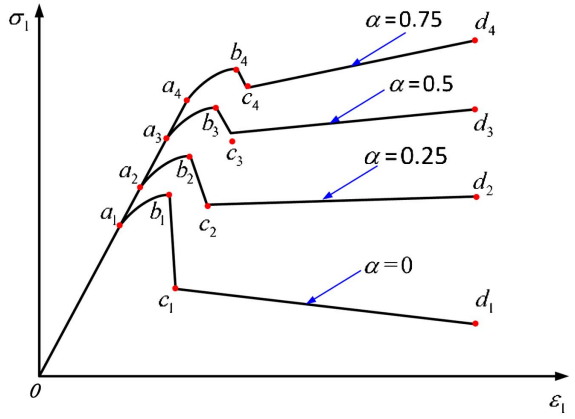

Fig. 5. Stress-strain curve under different confining pressures.

Fig. 7 clearly indicates that, for a given density, confining pressure has limited influence on elastic modulus, in agreement with previous findings (Lim and Ozbakkaloglu 2014; Zhou et al. 2016; Guo et al. 2015; Ansari and Li 1998; Binici 2005; Xiao et al. 2010). In contrast, significant positive correlation between density and elastic modulus is shown. The average elastic moduli for 250-, 450- and 650-kg/m^3 density are 106.21, 529.50, and 857.07 MPa, respectively, which indicates a clear monotonic trend. To further analyze the relationship between elastic modulus and density, a model proposed by Tan et al. (2017b) was used, expressed as follows:

$$E_0 = 133.13 \times (1.0029)^{\rho} \quad (7)$$

where E_0 = elastic modulus of the foamed concrete.

According to Eq. (7), Tan et al.'s elastic moduli for densities of 250, 450, and 650 kg/m^3 are 274.59, 534.45, and 874.45 MPa, respectively. In comparing these densities with those in this study (106.21, 529.50, and 857.07 MPa, respectively), it was found that Eq. (7) can well predict the elastic modulus for 450 and 650 kg/m^3 but not for 250 kg/m^3. This may be because, as stated in Tan et al. (2017b), the model is only suitable for foamed concrete with densities ranging 300–1,000 kg/m^3, which may mean that the elastic modulus of foamed concrete with a density of less than 300 kg/m^3 density must be treated differently.

As an alternative, the data from this study and those from Tan et al. (2017b) were combined. It was found that a linear fitting equation is more suitable for this combined data set, which can be seen in Fig. 8. The variation in elastic modulus with density can be expressed as

$$E_0 = 1.9572\rho - 370.41 \quad (8)$$

Peak Strain

The variation in average peak strain with confining pressure for all three densities is shown in Fig. 9. It can be observed that, for a given density, peak strain increases with confining pressure in a trend that is identical for all densities. When $\alpha = 0$, average peak strain for 250, 450, and 650 kg/m^3 is respectively 0.41, 0.32, and 0.39%, whereas when $\alpha = 0.75$, average peak strain almost doubles, to 0.81, 0.71, and 0.84%. In addition, with increasing confining pressure, the growth rate of peak strain slows down.

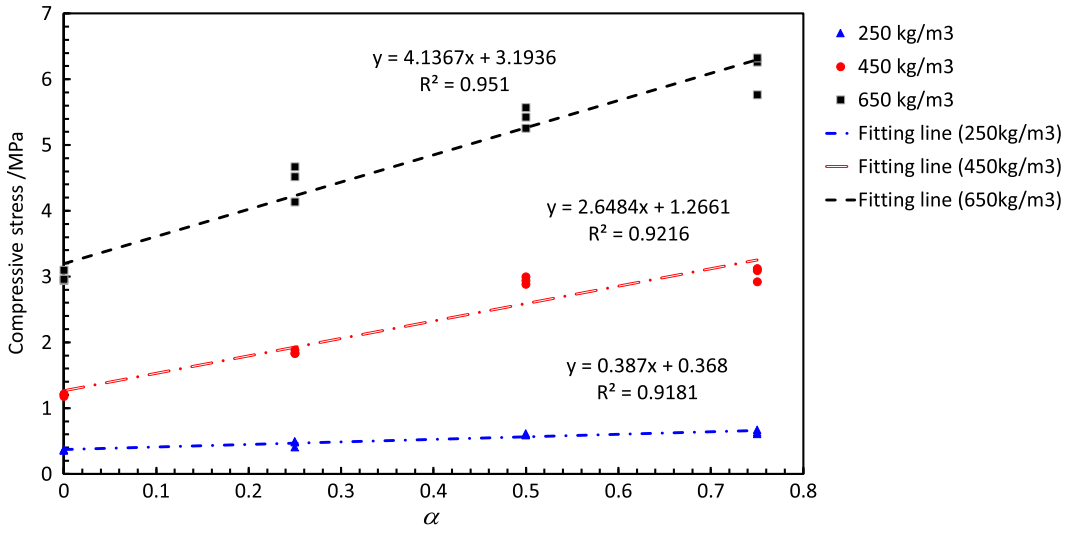

Fig. 6. Variation in peak stress (or compressive strength) with density and confining pressure.

Table 2. Values of k_1 and σ_c for different densities

	Density (kg/m^3)		
Parameter	250	450	650
k_1	0.387	2.6484	4.1367
σ_c	0.368	1.2661	3.1936

Using 250-kg/m^3 density as an example, when $\alpha = 0.25$ and 0.5, the corresponding peak strain is 0.72 and 0.79%. This means that, when α increases from 0 to 0.25, peak strain increases by 73.4% but when α increases from 0.25 to 0.5, peak strain increases by only 9.8%; when peak strain increases from 0.5 to 0.75, peak strain increases even more slowly, to 3.4%.

No significant correlation was detected between peak strain and density, the reason for which is explored in the section "Discussion."

Post-Peak Stress-Strain Relationship

As stated earlier, one of the key objectives of this research was to investigate the post-peak stress-strain characteristics of foamed concrete under large deformation. To this end, the post-peak stress-strain experimental data (Figs. 2–4) were analyzed in detail. A linear relationship between residual compressive strength and strain for almost all test cases was uncovered. Therefore, a linear function was employed to fit the data.

$$\sigma_{\text{post}} = k_2\varepsilon + \sigma_{re} \tag{9}$$

where σ_{post} = poststress (i.e., stress from Point c_i to Point d_i in Fig. 5); k_2 = slope of poststress with strain; and σ_{re} = residual stress (i.e., stress of Point c_i in Fig. 5). Both k_2 and σ_{re} are influenced by density and confining pressure, as summarized in Table 3.

The fitting results of the proposed model are shown in Fig. 10. They indicate that the prediction model reflects the experimental phenomena and trends. Furthermore, together with Table 3 and Fig. 9, we observe that, for all three densities, the value of k_2 is almost always positive except for $\alpha = 0$ (i.e., uniaxial compression) and there is a clear trend of increasing k_2 as α increases. This means that, unlike NWC and LWC, foamed concrete relatively easily maintains sufficiently high residual compressive strength under multiaxial loading (Persson 2001; Nematzadeh et al. 2016; Wu et al. 2017;

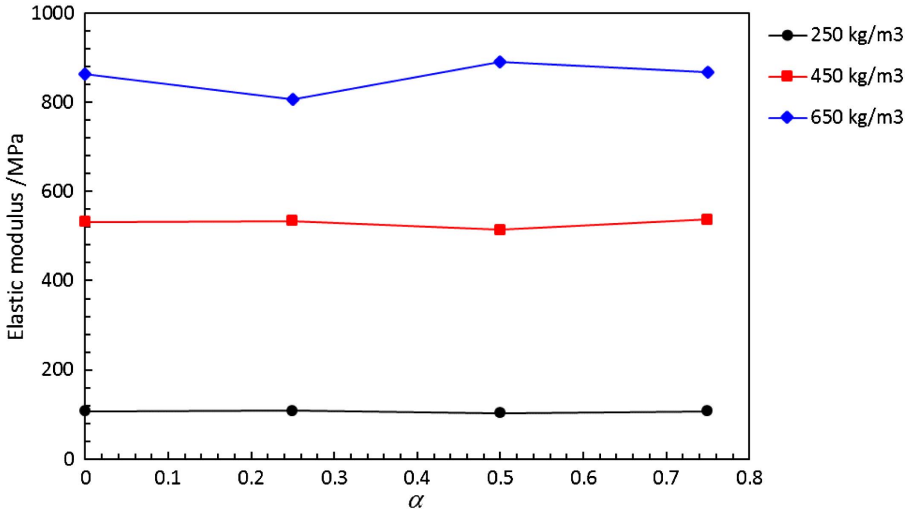

Fig. 7. Variation in elastic modulus with confining pressure for all densities.

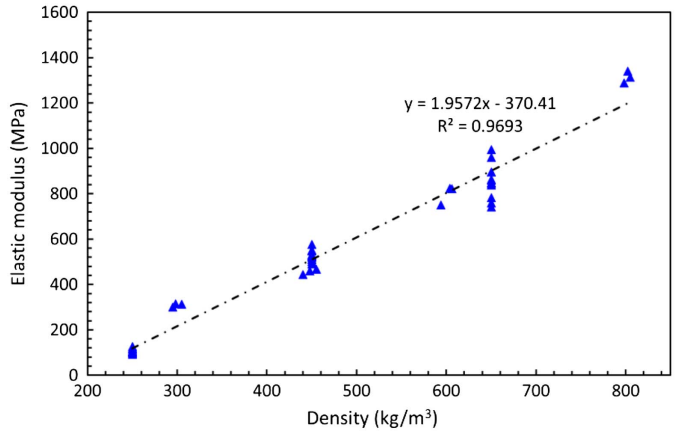

Fig. 8. Variation in elastic modulus with density. (Data from Tan et al. 2017b.)

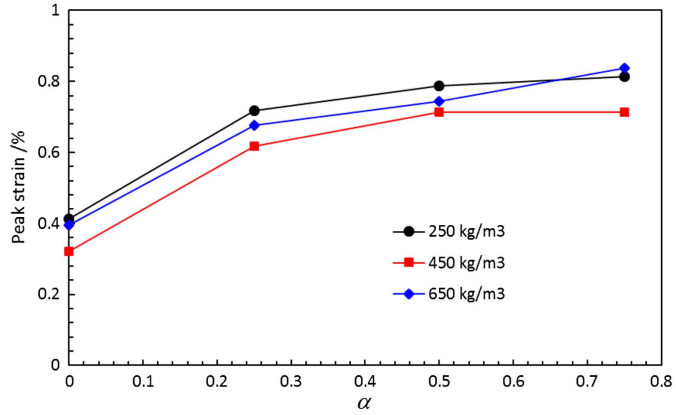

Fig. 9. Variation in peak strain with confining pressure for all densities.

Table 3. Variation in k_2 and σ_{re} at different densities and confining pressures

Model	Mix code	α	Coefficients k_2	Coefficients σ_{re}	R^2
$\sigma_{post} = k_2\varepsilon + \sigma_{re}$	M1	0	−0.5565	0.2098	0.73
		0.25	0.7542	0.3962	0.64
		0.5	1.035	0.4635	0.72
		0.75	1.1147	0.4706	0.85
	M2	0	−2.0858	0.5993	0.75
		0.25	1.5647	1.154	0.55
		0.5	2.3635	2.3175	0.90
		0.75	2.6377	2.9843	0.85
	M3	0	−5.2425	0.7927	0.89
		0.25	2.7327	4.1635	0.63
		0.5	8.2694	5.2129	0.71
		0.75	10.095	5.7412	0.86

Jiang et al. 2017; Gabet et al. 2008; Attard and Setunge 1996; Wee et al. 1996; Lim and Ozbakkaloglu 2014; Zhou et al. 2016). This makes it suitable for as a damping or energy-absorbing material. However, the proposed regression equations, based on three samples for each parameter in Table 3, may not be conclusive and should be considered only to indicate a general trend.

Discussion

Peak Strain

According to traditional understanding, the higher the density, the more brittle the concrete and the smaller the peak strain. However, the experimental results in Fig. 9 do not show significant correlation between peak strain and density. There are at least two probable reasons for this result, which was not expected.:

- The difference in brittleness for densities of 250–600 kg/m^3 was limited, and was not significant enough to be distinguished from experimental error; and
- Because the confining pressure was designated by a scale parameter, α, and not by absolute values, interpretation of the results became more difficult.

As a matter of fact, the experimental data reflected the relationship between brittleness and density in another way. As shown in Fig. 5, if the difference between b_i and c_i determines brittleness, it can be observed that, with increasing density, brittleness increases, which is shown by comparison of Figs. 2(a), 3(a), and 4(a).

Limit Strain

As mentioned before, one of the main advantages of foamed concrete is that it retains sufficiently high residual compressive strength under large deformation, making it suitable as a damping or energy-absorbing material. Limit strain is a key index to large deformation capability. Fig. 11 shows the relationship between limit strain and density under varying confining pressure.

From Fig. 11, it can be seen that (1) when $\alpha = 0$, the limit strain for all three densities is almost the same; and (2) when the samples are under triaxial compression, the foamed concrete with 450-kg/m^3 density always has the highest limit strain. That is to say, foamed concrete of approximately 450-kg/m^3 density is probably most suitable for use as a damping or energy-absorbing material if its compressive strength and other properties can satisfy engineering requirements.

Conclusions

In order to investigate the stress-strain characteristics of foamed concrete subjected to axial strain greater than 10% under uniaxial and triaxial compressive loading, foamed concrete specimens at three different densities (250, 450, and 650 kg/m^3) were tested using a servocontrolled testing machine. Axial stress-strain (σ_1-ε) curves were obtained, and peak stress (compressive strength), elastic modulus, peak strain, and the postpeak stress-strain relationship were analyzed. According to the analysis results, the following conclusions can be drawn:

- The stress-strain characteristics at all three densities are similar and can be idealized as four stages: elastic deformation, plastic deformation, postpeak strain softening, and residual deformation;
- Compressive strength increases as density and confining pressure increase;the linear fitting equation to describe the quantitative relationships among these parameters is $\sigma_{peak} = k_1 \cdot \alpha + \sigma_c$;
- For a given density, confining pressure has limited influence on elastic modulus, but there is significant positive correlation between density and elastic modulus,expressed as $E_0 = 1.9572\rho - 370.41$;
- No significant correlation can be detected between peak strain and density, but peak strain increases as confining pressure increases; and
- A linear relationship between residual compressive strength and strain exists for almost all of the test cases; based on the

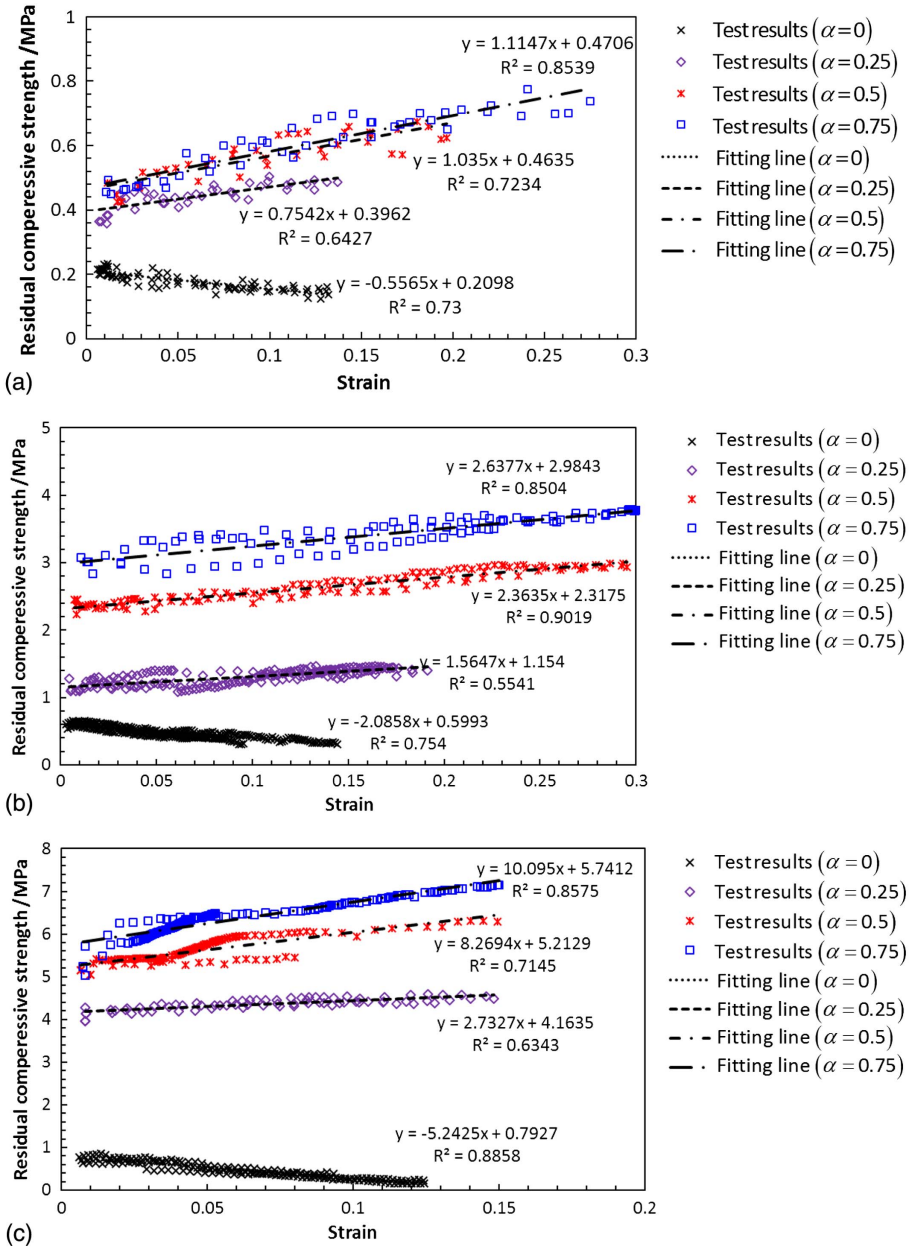

Fig. 10. Comparison of results between Eq. (9) and experimental data at different densities: (a) 250 kg/m^3; (b) 450 kg/m^3; and (c) 650 kg/m^3.

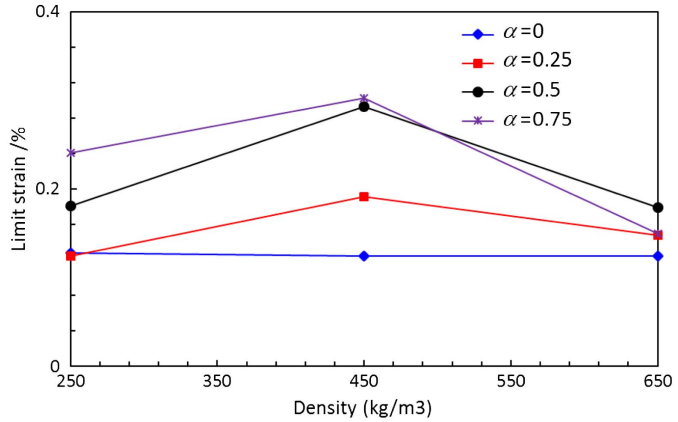

Fig. 11. Relationship between limit strain and density at different confining pressures.

experimental results, a linear function to fit the data is given as $\sigma_{\text{post}} = k_2\varepsilon + \sigma_{re}$.

As mentioned in the "Introduction," mix design has an important effect on the behavior of foamed concrete. Because only one mix design was tested, it is difficult to know how general the findings are and how robust the observed trends are across materials. For these reasons, more and broader research is needed to produce concretes with varying peak strengths independent of density.

Acknowledgments

This work was supported by the National Program on Key Basic Research Project (973 Program) (Grant No. 2015CB057906), the National Natural Science Foundation of China (Grant Nos. 51208499 and 51579238), the Postdoctoral Science Foundation of China (Grant Nos. 2014M550365 and 2015T80718), the Chinese

Scholarship Council, and the Youth Innovation Promotion Association CAS.

References

Ahmad Zaidi, A. M., and Q. M. Li. 2009. "Investigation on penetration resistance of foamed concrete." *Proc. Inst. Civ. Eng. Struct. Build.* 162 (1): 77–85. https://doi.org/10.1680/stbu.2009.162.1.77.

Alexanderson, J. 1979. "Relations between structure and mechanical properties of autoclaved aerated concrete." *Cem. Concr. Res.* 9 (4): 507–514. https://doi.org/10.1016/0008-8846(79)90049-8.

Amran, Y. H. M., N. Farzadnia, and A. A. A. Ali. 2015. "Properties and applications of foamed concrete: A review." *Constr. Build. Mater.* 101 (1): 990–1005. https://doi.org/10.1016/j.conbuildmat.2015.10.112.

Ansari, F., and QB. Li. 1998. "High-strength concrete subjected to triaxial compression." *ACI Mater. J.* 95 (6): 747–755.

Attard, M. M., and S. Setunge. 1996. "Stress-strain relationship of confined and unconfined concrete." *ACI Mater. J.* 93 (5): 432–442.

Binici, B. 2005. "An analytical model for stress-strain behavior of confined concrete." *Eng. Struct.* 27 (7): 1040–1051. https://doi.org/10.1016/j.engstruct.2005.03.002.

Chen, B., Z. Wu, and N. Liu. 2012. "Experimental research on properties of high-strength foamed concrete." *J. Mater. Civ. Eng.* 24 (1): 113–118.

Chen, X., S. Wu, and J. Zhou. 2013. "Influence of porosity on compressive and tensile strength of cement mortar." *Constr. Build. Mater.* 40 (3): 869–874. https://doi.org/10.1016/j.conbuildmat.2012.11.072.

Gabet, T., Y. Malécot, and L. Daudeville. 2008. "Triaxial behaviour of concrete under high stresses: Influence of the loading path on compaction and limit states." *Cem. Concr. Res.* 38 (3): 403–412. https://doi.org/10.1016/j.cemconres.2007.09.029.

Guo, H., W. Guo, and Y. Shi. 2015. "Computational modeling of the mechanical response of lightweight foamed concrete over a wide range of temperatures and strain rates." *Constr. Build. Mater.* 96: 622–631. https://doi.org/10.1016/j.conbuildmat.2015.08.064.

Hoff, G. C. 1972. "Porosity-strength considerations for cellular concrete." *Cem. Concr. Res.* 2 (1): 91–100. https://doi.org/10.1016/0008-8846(72)90026-9.

Jiang, C., Y. F. Wu, and J. F. Jiang. 2017. "Effect of aggregate size on stress-strain behavior of concrete confined by fiber composites." *Compos. Struct.* 168: 851–862. https://doi.org/10.1016/j.compstruct.2017.02.087.

Jones, M. R. 2001. "Foamed concrete for structural use." In *Proc., One Day Seminar on Foamed Concrete: Properties, Applications and Latest Technological Developments*, 27–60. Loughborough, UK: Loughborough Univ.

Jones, M. R., and A. McCarthy. 2005. "Preliminary views on the potential of foamed concrete as a structural material." *Mag. Concr. Res.* 57 (1): 21–31. https://doi.org/10.1680/macr.2005.57.1.21.

Jones, M. R., and L. Zheng. 2013. "Energy absorption of foamed concrete from low-velocity impacts." *Mag. Concr. Res.* 65 (4): 209–219. https://doi.org/10.1680/macr.12.00054.

Kearsley, E. P., and P. J. Wainwright. 2002. "The effect of porosity on the strength of foamed concrete." *Cem. Concr. Res.* 32 (2): 233–239. https://doi.org/10.1016/S0008-8846(01)00665-2.

Kearsley, E. P., and P. J. Wainwright. 2011. "The effect of high fly ash content on the compressive strength of foamed concrete." *Cem. Concr. Res.* 31 (1): 105–112. https://doi.org/10.1016/S0008-8846(00)00430-0.

Kim, H. K., and H. K. Lee. 2011. "Use of power plant bottom ash as fine and coarse aggregates in high-strength concrete." *Constr. Build. Mater.* 25 (2): 1115–1122. https://doi.org/10.1016/j.conbuildmat.2010.06.065.

Li, L., and J. Purkiss. 2005. "Stress-strain constitutive equations of concrete material at elevated temperatures." *Fire Saf. J.* 40 (7): 669–686. https://doi.org/10.1016/j.firesaf.2005.06.003.

Lian, C., Y. Zhuge, and S. Beecham. 2011. "The relationship between porosity and strength for porous concrete." *Constr. Build. Mater.* 25 (11): 4294–4298. https://doi.org/10.1016/j.conbuildmat.2011.05.005.

Lim, J. C., and T. Ozbakkaloglu. 2014. "Stress-strain model for normal-and light-weight concretes under uniaxial and triaxial compression." *Constr. Build. Mater.* 71: 492–509. https://doi.org/10.1016/j.conbuildmat.2014.08.050.

Ma, C., and B. Chen. 2015. "Properties of a foamed concrete with soil as filler." *Constr. Build. Mater.* 76: 61–69. https://doi.org/10.1016/j.conbuildmat.2014.11.066.

Mydin, M. A. O.. 2012. "Characterization of high temperature modulus of elasticity of lightweight foamed concrete under static flexural and compression: An experimental investigations." *Eur. Res.* 30 (9-3): 1545–1553. https://doi.org/10.1016/j.conbuildmat.2016.02.180.

Mydin, M. A. O., and Y. C. Wang. 2012. "Mechanical properties of foamed concrete exposed to high temperatures." *Constr. Build. Mater.* 26 (1): 638–654. https://doi.org/10.1016/j.conbuildmat.2011.06.067.

Narayanan, N., and K. Ramamurthy. 2000. "Structure and properties of aerated concrete: A review." *Cem. Concr. Compos.* 22 (5): 321–329. https://doi.org/10.1016/S0958-9465(00)00016-0.

National Standard of the People's Republic of China. 2007. *Portland cement and ordinary portland cement*. GB175-2007. Beijing: China Communication Press.

Nematzadeh, M., A. Salari, J. Ghadami, and M. Naghipour. 2016. "Stress-strain behavior of freshly compressed concrete under axial compression with a practical equation." *Constr. Build. Mater.* 115: 402–423. https://doi.org/10.1016/j.conbuildmat.2016.04.045.

Othuman, M. A., and Y. C. Wang. 2011. "Elevated-temperature thermal properties of lightweight foamed concrete." *Constr. Build. Mater.* 25 (2): 705–716. https://doi.org/10.1016/j.conbuildmat.2010.07.016.

Pan, Z., F. Hiromi, and T. Wee. 2007. "Preparation of high performance foamed concrete from cement, sand and mineral admixtures." *J. Wuhan Univ. Technol.* 22 (2): 295–298. https://doi.org/10.1007/s11595-005-2295-4.

Persson, B. 2001. "A comparison between mechanical properties of self-compacting concrete and the corresponding properties of normal concrete." *Cem. Concr. Res.* 31 (2): 193–198. https://doi.org/10.1016/S0008-8846(00)00497-X.

Qiao, X. C., B. R. Ng, M. Tyrer, C. S. Poon, and C. R. Cheeseman. 2008. "Production of lightweight concrete using incinerator bottom ash." *Constr. Build. Mater.* 22 (4): 473–480. https://doi.org/10.1016/j.conbuildmat.2006.11.013.

Ramamurthy, K., E. K. K. Nambiar, and G. I. S. Ranjani. 2009. "A classification of studies on properties of foamed concrete." *Cem. Concr. Compos.* 31 : 388–396.

Rößler, M., and I. Odler. 1985. "Investigations on the relationship between porosity, structure and strength of hydrated portland cement pastes. I: Effect of porosity." *Cem. Concr. Res.* 15 (3): 401–410.

Sayadi, A. A., J. V. Tapia, T. R. Neitzert, and G. C. Clifton. 2016. "Effects of expanded polystyrene (EPS) particles on fire resistance, thermal conductivity and compressive strength of foamed concrete." *Constr. Build. Mater.* 112: 716–724. https://doi.org/10.1016/j.conbuildmat.2016.02.218.

Shafigh, P, M. Z. Jumaat, H. B. Mahmud, and U. J. Alengaram. 2011. "A new method of producing high strength oil palm shell lightweight concrete." *Mater. Des.* 32 (10): 4839–4843. https://doi.org/10.1016/j.matdes.2011.06.015.

Sim, J. I., K. H. Yang, H. Y. Kim, and B. J. Choi. 2013. "Size and shape effects on compressive strength of lightweight concrete." *Constr. Build. Mater.*, 38 (2): 854–864. https://doi.org/10.1016/j.conbuildmat.2012.09.073.

Soleimanzadeh, S., and M. A. O. Mydin. 2013. "Influence of high temperatures on flexural strength of foamed concrete containing fly ash and polypropylene fiber." *Int. J. Eng.* 26 (1): 365–374. https://doi.org/10.5829/idosi.ije.2013.26.02b.02.

Tan, X., W. Chen, Y. Hao, and X. Wang. 2014. "Experimental study of ultralight (<300 kg/m^3) foamed concrete." *Adv. Mater. Sci. Eng.* 2014: 1. https://doi.org/10.1155/2014/514759.

Tan, X., W. Chen, H. Liu, A. H. Chan, H. Tian, X. Meng, F. Wang, and X. Deng. 2017a. "A combined supporting system based on foamed concrete and U-shaped steel for underground coal mine roadways undergoing large deformations." *Tunnelling Underground Space Technol.* 68 (68): 196–210. https://doi.org/10.1016/j.tust.2017.05.023.

Tan, X., W. Chen, H. Tian, and J. Yuan. 2013. "Degradation characteristics of foamed concrete with lightweight aggregate and polypropylene fibre under freeze-thaw cycles." *Mag. Concr. Res.* 65 (12): 720–730. https://doi.org/10.1680/macr.12.00145.

Tan, X., W. Chen, J. Wang, D. Yang, X. Qi, Y. Ma, X. Wang, S. Ma, and C. Li. 2017b. "Influence of high temperature on the residual physical and mechanical properties of foamed concrete." *Constr. Build. Mater.* 135: 203–211. https://doi.org/10.1016/j.conbuildmat.2016.12.223.

Tian, T., Y. Yan, Z. Hu, Y. Xu, Y. Chen, and J. Shi. 2016. "Utilization of original phosphogypsum for the preparation of foamed concrete." *Constr. Build. Mater.* 115: 143–152. https://doi.org/10.1016/j.conbuildmat.2016.04.028.

Tikalsky, P. J., J. Pospisil, and W. MacDonald. 2014. "A method for assessment of the freeze-thaw resistance of preformed foam cellular concrete." *Cem. Concr. Res.* 34 (5): 889–893. https://doi.org/10.1016/j.cemconres.2003.11.005.

Wang, H., W. Z. Chen, X. J. Tan, H. M. Tian, and J. J. Cao. 2012. "Development of a new type of foamed concrete and its application on stability analysis of large-span soft rock tunnel." *J. Cent. South Univ.* 19 (11): 3305–3310. https://doi.org/10.1007/s11771-012-1408-4.

Wee, T. H., M. S. Chin, and M. A. Mansur. 1996. "Stress-strain relationship of high-strength concrete in compression." *J. Mater. Civ. Eng.* 8 (2): 70–76. https://doi.org/10.1061/(ASCE)0899-1561(1996)8:2(70).

Wu, J., X. Jing, and Z. Wang. 2017. "Uni-axial compressive stress-strain relation of recycled coarse aggregate concrete after freezing and thawing cycles." *Constr. Build. Mater.* 134: 210–219. https://doi.org/10.1016/j.conbuildmat.2016.12.142.

Xiao, Q. G., J. G. Teng, and T. Yu. 2010. "Behavior and modeling of confined high-strength concrete." *J. Compos. Constr.* 14 (3): 249–259. https://doi.org/10.1061/(ASCE)CC.1943-5614.0000070.

Yap, S. P., U. J. Alengaram, and M. Z. Jumaat. 2013. "Enhancement of mechanical properties in polypropylene-and nylon-fibre reinforced oil palm shell concrete." *Mater. Des.* 49: 1034–1041. https://doi.org/10.1016/j.matdes.2013.02.070.

Zhang, Z. Q., J. L. Yang, and Q. M. Li. 2013. "An analytical model of foamed concrete aircraft arresting system." *Int. J. Impact Eng.* 61: 1–12. https://doi.org/10.1016/j.ijimpeng.2013.05.006.

Zhou, Y., X. Liu, F. Xing, H. Cui, and L. Sui. 2016. "Axial compressive behavior of FRP-confined lightweight aggregate concrete: An experimental study and stress-strain relation model." *Constr. Build. Mater.* 119: 1–15. https://doi.org/10.1016/j.conbuildmat.2016.02.180.